# A comparative study of $Nd^{3+}$ and $Sm^{3+}$ ions doped into oxide host materials; correlation between structure and spectral properties

C. GHEORGHE*, A. LUPEI, V. LUPEI, L. GHEORGHE
*National Institute for Laser, Plasma and Radiation Physics, ECS Laboratory, 077125, Magurele – Bucharest, Romania*

The $Nd^{3+}$ and $Sm^{3+}$ spectroscopic characteristics (energy levels and emission wavelengths) dependences on the host structure and composition are analyzed. These ions are interesting for visible emission: blue obtained by doubling the $Nd^{3+}$ laser emission in 900 nm range and orange –red by direct pumping of $Sm^{3+}$ ion. The hosts are different oxide materials: sesquioxides ceramics $Y_2O_3$, $Sc_2O_3$, garnet ceramics $Y_3Al_5O_{12}$ – YAG and hexaaluminates $Sr_{1-x}La_xMg_xAl_{12-x}O_{19}$ – ASL single crystals. The data are discussed in terms of the nephelauxetic effect and the crystal field strengths. The role of both effects on the emission wavelengths is outlined.

(Received October 17, 2011; accepted February 20, 2012)

*Keywords*: Oxide laser materials, $Nd^{3+}$, $Sm^{3+}$, Dopant – host correlation

## 1. Introduction

The lasers or phosphors emitting efficiently in visible are required for many applications: technological, military, telecommunication- marine, display, phosphors, biomedicine, etc and the search of new systems is active. Emission in this wavelength range can be obtained either by direct emission from doped materials or by nonlinear processes of volume (from the infrared fundamental radiation of solid-state lasers in a non-linear crystal), and atomic processes (energy transfer or multiple step absorptions). Either solution imply well-definite emission wavelength determined by the energy levels and optical transition probabilities specific to each active ion and each host environment. Among host, the inorganic materials (single crystals, ceramics, etc) doped with rare earth - $RE^{3+}$ ions represent important classes. In the last years the most investigated inorganic laser materials, especially for infrared emission, are the cubic transparent ceramics (garnets or sesquioxides) mainly doped with $Nd^{3+}$ or $Yb^{3+}$.

Important steps for the extension of wavelengths of the emitting sources are the spectroscopic studies of the processes determining the emission characteristics. When a $RE^{3+}$ ion is embedded in a solid matrix, the static interaction between the dopant ion and its neighbors are determining both the structure of the energy levels and the probabilities of the optical transitions. The main factors influencing the energy levels of the $RE^{3+}$ ion in a host are the *nephelauxetic effect* (the movement of electronic configuration, the spectral terms and positions of electronic levels of free ion in a given matrix) and the *interaction with the crystalline field* [1 - 3]. The crystal field interaction depends on the nature of the $RE^{3+}$ ion and the composition and material structure (nature, valence and ligands number from the first anionic coordination sphere, the cation - anion distance, local symmetry and geometry of the position occupied by $RE^{3+}$ ions) and determine the Stark splitting of the energy levels**,** raising totally or partially the degeneration of the free ion levels. Though the crystal field interaction is dominated by the first anionic coordination sphere (nearest), the more distant coordination spheres, including cationic ones are contributing too [4].

The visible emission of $RE^{3+}$ by direct pumping is less efficient either due to pumping difficulties or luminescence quenching processes, and has been insufficiently studied for many years. However, one should mention the increased recent interest in $Sm^{3+}$ or $Dy^{3+}$ ions (that present strong emissions in visible, with long lifetimes at low concentrations) mainly due to the tremendous development of UV/VIS laser diodes in the last years. The blue emission of these ions is rather inefficient. The stronger emissions are in orange red ($Sm^{3+}$) and yellow ($Dy^{3+}$).

The blue laser emission, required for different applications, has been obtained by the frequency doubling in a non-linear crystal of the infrared 900-950 nm quasi-three-level $^4F_{3/2} \rightarrow {}^4I_{9/2}$ emission of $Nd^{3+}$ in various materials. The position of the $Nd^{3+}$ $^4F_{3/2}$ metastable level and splitting of the $^4I_{9/2}$ fundamental level allow the laser at different wavelengths: ~966 nm in $Sc_2O_3$ [5], ~ 946 nm in $Y_2O_3$ [6], ~ 946 nm in YAG [7-9], or ~ 901 nm in strontium lanthanum aluminates $Sr_{1-x}Nd_yLa_{x-y}Mg_xAl_{12-x}O_{19}$ (ASL: Nd) crystals [10,11].

The purpose of this paper is to present a correlation between the emission wavelengths of $Nd^{3+}$ in the 900 nm range with the structural and compositional characteristics of the host. The chosen hosts are cubic transparent ceramics: garnets- $Y_3Al_5O_{12}$ (YAG) and sesquioxides - $Y_2O_3$ and $Sc_2O_3$ and strontium lanthanum hexaaluminate

(ASL) single crystals. A similar analysis was performed for $Sm^{3+}$ in the same hosts.

## 2. Results and discussion

The analysis that shall be presented is based mainly on our experimental data published previously. All the matrices chosen in this investigation are oxides, but the $RE^{3+}$ ions are placed in sites with different oxygen coordination number (CN) and local symmetry, a fact that influence strongly the energy level structure and transition probabilities. Thus, in sesquioxides ($Y_2O_3$, $Sc_2O_3$ ) that belongs to cubic bixbyite structure with spatial group Ia3, the cations $Y^{3+}$ or $Sc^{3+}$ occupy two types of sites with $C_2$ and $C_{3i}$ local symmetry in a ratio of 3/1 and the with 6 $O^{2-}$ as near neighbors in both sites [12]. $RE^{3+}$ could enter in both sites, but the optical spectra are dominated by centers with $C_2$ local symmetry, since the inversion symmetry of $C_{3i}$ centers preclude the electric -dipole transitions. The $RE^{3+}$ ions in YAG (space group $IA\bar{3}$) enter in garnet dodecahedral sites occupied by $Y^{3+}$ having 8 $O^{2-}$ as near neighbors and $D_2$ local symmetry [12]. The $Sr_{1-x}Nd_yLa_{x-y}Mg_xAl_{12-x}O_{19}$ - ASL crystals have hexagonal magnetoplumbite structure and offer for substitution with $RE^{3+}$ a unique $Sr^{2+}$ (2d) site of ideal $D_{3h}$ symmetry, with 12 $O^{2-}$ coordination [12]. Some structural data for the matrices used in this analysis are given in Table 1.

*Table 1. Important structural factors that influence the nephelauxetic and crystal field effects.*

| | **$Sc_2O_3$** | **$Y_2O_3$** | **YAG** | **ASL** |
|---|---|---|---|---|
| System type | Cubic | Cubic | Cubic | Hexagonal |
| Symmetry of cationic sites | $C_2$ | $C_2$ | $D_2$, $C_{3i}$, $S_4$ | $D_{3h}$ |
| Substituted cation | $Nd^{3+}$/ $Sc^{3+}$ | $Nd^{3+}$/ $Y^{3+}$ | $Nd^{3+}$/ $Y^{3+}$ | $Nd^{3+}$/ $La^{3+}$/ $Sr^{2+}$ |
| Ionic Radii [13] | 0.98 Å/ 0.75 Å | 0.98 Å/ 0.9 Å | 1.1Å/ 1.02Å | 1.27 Å/ 1.32 Å/ 1.4Å |
| Coordination number (CN- $O^{2-}$) | 6 | 6 | 8 | 12 |
| Cation- - anion distances | 2.09- 2.17 Å | 2.24- 2.75 Å | 2.3- 2.36Å | 2.69- 2.84 Å |
| Cation – cation distances (near neighbor sphere) | 4 × 3.26 Å | 4 × 3.52 Å | 4 × 3.67Å | 6 × 5.56 Å |
| Cation – cation distances (next 2 cationic sphere) | 8 × 3.28 Å | 8 × 3.53 Å | 8 × 5.12Å | 6 × 9.62 Å |

In the sites with local symmetry ($C_2$, $D_2$, $D_{3h}$) occupied by $Nd^{3+}$, the $^{2S+1}L_J$ manifolds are split in (2J+1)/2 Kramers doublets. The Stark energy levels of $Nd^{3+}$ in ceramic samples ($Nd^{3+}$ in $D_2$ sites in YAG [14, 15], $Nd^{3+}$ in $C_2$ sites in $Y_2O_3$ [16, 17] or $Sc_2O_3$ [18, 19) are similar to the previous data on single crystals [3, 20]. The high-resolution optical spectroscopy [21, 22] of ASL: Nd for $0.2 \le x \le 0.4$, $0.05 \le y \le 0.15$ revealed the clear presence of two types of structural centers, $C_1$ and $C_2$, whose proportion is determined by the composition parameter x: $C_1$ dominates at high x, while $C_2$ has large concentrations only at low x values, they have different energy levels schemes, the $C_1$ si $C_2$ centers have the same 12 $O^{2-}$ vicinity, but as composition dependence and polarization data show, only center $C_2$ has $D_{3h}$ symmetry, $C_1$ differs by nearby cationic vicinity that influence the energy levels positions and local symmetry.

### 2.1 $Nd^{3+}$ ion in oxides

As metioned above the energy levels structure of a RE ion in a matrix is dependent on nephelauxetic effect and crystal field strengths. The nephelauxetic effect [1, 2], i.e. the modification of the "free ion" parameters by expansion of the electronic cloud of the dopant ion is mainly due to the covalent bonds with ligands, leading to decreasing of the electron - electron interactions and spin – orbit coupling. These changes determine the movement of electronic configuration, the spectral terms and positions of electronic levels of the free ion in solid matrices. The nephelauxetic effect is determined essentially by the nature of the ion and first coordination anionic sphere. The materials have a very important role by the ions in the first coordination sphere: *i*) the anion type and the covalent bonding; *ii*) the number of anions; *iii*) cation-anion distances; *iv*) the geometry, etc. In the case of $RE^{3+}$ ions in solid matrices the barycenters positions of the manifolds are influenced by the nephelauxetic effect. The barycenters of the $^{2S+1}L_J$ manifolds are defined as Bc ($^{2S+1}L_J$) = E ($^{2S+1}L_J$) – $E_0$, where E is average energy of Stark split levels of the $^{2S+1}L_J$ excited manifold and $E_0$ that of the ground manifold. In Table 2 the barycenters of the $^4F_{3/2}$ $Nd^{3+}$ metastable level function on the host structure are given, as could be observed they are shifted toward higher energies as the CN oxygen coordination (near neighbors) numbers increase.

A very illustrative way to represent the material structural and compositional effects on the energy levels of $RE^{3+}$ ions are the barycenter curves [24], as illustrated in Fig. 1, where one observe that the barycenters the $^4F_{3/2}$ and $^2P_{1/2}$ of $Nd^{3+}$ determined from experimental data for different matrices included GdCOB [25] align well on a straight line. The points shift at low energy with the decrease of oxygen coordination number and relative to the energy levels of the free $Nd^{3+}$ ion.

*Table 2. The dependence of the $^4F_{3/2}$ $Nd^{3+}$ barycenters on the host structure.*

| | $Sc_2O_3$ | $Y_2O_3$ | YAG | ASL | $Nd^{3+}$ free ion [23] |
|---|---|---|---|---|---|
| Symmetry of cationic sites | $C_2$ | $C_2$ | $D_2$ | $D_{3h}$ | |
| CN | 6 | 6 | 8 | 12 | |
| Substituted cation | $Sc^{3+}$/ $Nd^{3+}$ | $Y^{3+}$/ $Nd^{3+}$ | $Y^{3+}$/ $Nd^{3+}$ | $Sr^{2+}$/ $Nd^{3+}$ | |
| $^4F_{3/2}$ $Nd^{3+}$ barycenter ($cm^{-1}$) | 10930 | 11022 | 11168 | 11375 | 11698 |

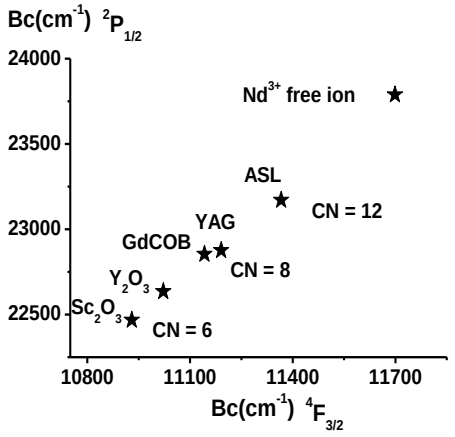


*Fig. 1. The barycenter positions of $^4F_{3/2}$ and $^2P_{1/2}$ $Nd^{3+}$ multiplets in different matrices. CN is the near neighbor oxygen coordination number*

The crystal field effects, manifested by the splitting in Stark levels of the $^{2S+1}L_J$ manifolds are dependent on local symmetry, coordination number, cation - anions or cation - cations distances, etc. This is illustrated in Fig. 2 where a partial energy level schemes for $Nd^{3+}$ in $C_2$ sites of $Y_2O_3$ or $Sc_2O_3$, $D_2$ sites in YAG and $D_{3h}$ sites in ASL center (center $C_2$ [22]) are given. The data revealed very different crystal field effects in strontium lanthanum aluminates ($Sr_{1-x}Nd_yLa_{x-y}Mg_xAl_{12-x}O_{19}$) and sesquioxides ($Sc_2O_3$, $Y_2O_3$). The coordination number and cation - anion distances are quite large in ASL and induce moderate crystal field effects on the $Nd^{3+}$ ion. For $Sc_2O_3$, $Y_2O_3$ sesquioxides, the coordination number, small cation - anion and cation - cation distances, determine strong crystal field effects, especially for $Sc_2O_3$.

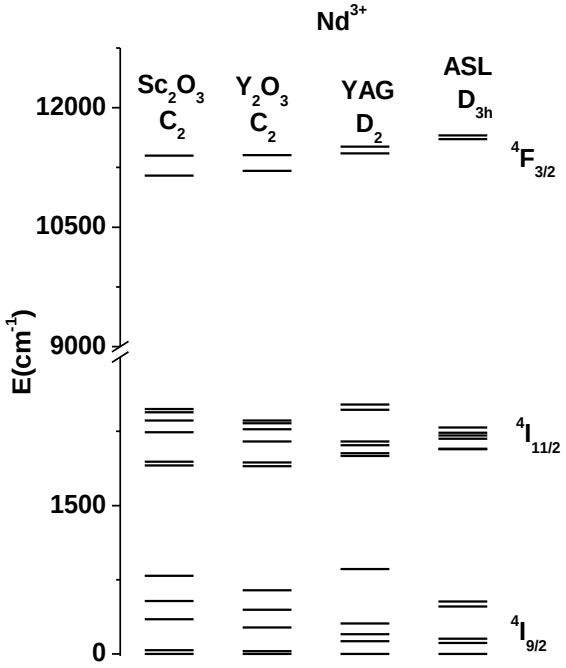


*Fig. 2. Partial energy level schemes of $Nd^{3+}$ in $Sc_2O_3$, $Y_2O_3$, YAG and ASL.*

To compare the effects of different hosts, a scalar parameter $N_V$ was introduced [26] –it is characteristic to the crystal field strength of any local symmetry. It could be calculated from the phenomenological crystal field parameters $B_q^k$ by the relation [25]

$$N_v = \left[ \sum_{k,q} \left(B_q^k\right)^2 \left( \frac{4\pi}{2k+1} \right) \right]^{1/2}$$

Using the published crystal field parameters $B_q^k$, $N_v$ parameter has been calculated for $Nd^{3+}$ in $C_2$ sites in $Y_2O_3$ [4], $Nd^{3+}$: YAG in $D_2$ sites [27] and $Nd^{3+}$: ASL $C_2$ centers $D_{3h}$ symmetry ($C_2$ centers) [28]. In Fig. 3 the maximum splittings $\Delta E(J)$ for $^4I_{9/2}$ and $^4F_{3/2}$ manifolds of the $Nd^{3+}$ ion function of $N_v$ parameter are given. One should mention that for estimation of $N_v$ one should take into account the selection rule $2J \geq k$. Therefore, for $^4I_{9/2}$ $\Delta E(J)$ splitting is compared with $N_v$ calculated with all $B_q^k$ parameters, while for J=3/2, only the parameters $B_q^k$ with k = 2 that determine the splitting of this manifold are considered. For both manifolds one could observe an almost linear dependence, but with different slopes. Besides, the data show that the second order parameters are larger in $Y_2O_3$ than in YAG.

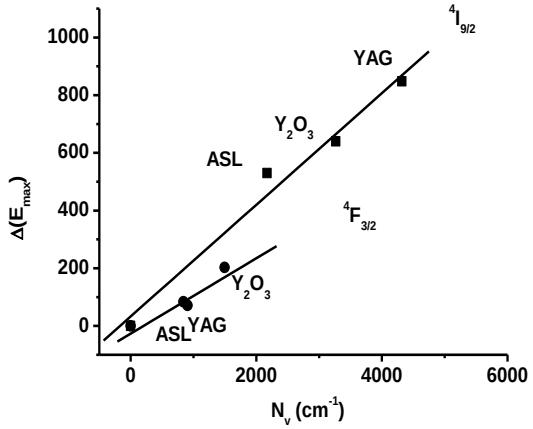


*Fig. 3. The maximum splitting of the $^4I_{9/2}$ and $^4F_{3/2}$ $Nd^{3+}$ manifolds function on the scalar parameter $N_v$.*

The laser emission of $Nd^{3+}$ in the 900 nm range comes from the transition $^4F_{3/2}$ (1) $\rightarrow ^4I_{9/2}$(5), where numbers denotes the Stark levels of the manifolds. Since such a laser works in a quasi- three level schemes, the terminal laser level should be high in energy to avoid the reabsorption of the laser emission. The emission wavelengths are at ~ 966 nm for Nd in $Sc_2O_3$ [5], at 946 nm for $Nd^{3+}$ in $Y_2O_3$ [6], 946 nm in YAG [7], or ~ 901nm in ASL [10]. Though the emission wavelengths decrease from $Sc_2O_3$ (~ 966 nm) to ASL (~ 901 nm) (Fig. 1, 2), according to nephelauxetic effect, the emission in YAG (~ 946 nm) is almost identical to that in $Y_2O_3$ (~ 946 nm) due to the stronger crystal field splitting of the $^4I_{9/2}$ manifold in YAG.

### 2.2 $Sm^{3+}$ ions in oxides

The $Sm^{3+}$ emission studies in various materials, especially for fosphors in orange –red range, but also for laser emission, has increased in the last years in connection with the development of lasers diodes in the 405 nm range, used already in many applications (lighting, optical storage, etc). There are, however, few systematic spectroscopic studies on $Sm^{3+}$ ion. Thus, the crystal field effects studies in the analyzed host refer to $Sm^{3+}$ in $Y_2O_3$ crystal [29] , in YAG crystal [30, 31] or YAG ceramic [32], in ASL crystals [33, 34] and in $Sc_2O_3$ [35].

The energy level structure of $Sm^{3+}$ ion contains a dense group of energy manifolds $^6H_J$ (with J from 5/2, the ground manifold, to 15/2) and $^6F_J$ (with J=1/2 to 11/2) extending to about ~ 10000 $cm^{-1}$, followed by an energy gap up to ~ 17000 $cm^{-1}$, above which there is again a dense packing of energy manifolds originating from the spectral terms $^4G$, $^4F$, $^4I$, $^4M$, etc, extending to UV [29], the lower one being the $^4G_{5/2}$ metastable level. As could be observed in Table 3 the position of barycenters of $^4G_{5/2}$ metastable level increses from $Sc_2O_3$ to ASL, giving the possibility of different emission wavelengths. The most intense emission lines of $Sm^{3+}$ correspond to spin forbidden transition $^4G_{5/2} \rightarrow ^6H_{7/2}$ (orange) and $^4G_{5/2} \rightarrow ^6H_{9/2}$ (red).

*Table 3. the barycenters of $Sm^{3+}$ $^4G_{5/2}$ manifold in different oxides.*

| | $Sc_2O_3$ | $Y_2O_3$ | YAG | ASL ($C_2$) |
|---|---|---|---|---|
| | CN = 6 | CN = 6 | CN=8 | CN = 12 |
| | $Sc^{3+}/Sm^{3+}$ | $Y^{3+}/Sm^{3+}$ | $Y^{3+}/Sm^{3+}$ | $Sr^{2+}/Sm^{3+}$ |
| $^4G_{5/2}$ $Sm^{3+}$ barycenter ($cm^{-1}$) | 17309 | 17479 | 17648 | 17865 |

The crystal fields effects on $Sm^{3+}$ in different hosts are illustrated in Fig. 4, where the Stark levels of the ground manifold and those involved in orange emission are given. The emission wavelengths decrease from $Sc_2O_3$ to ASL with exception of YAG. Thus, $Sm^{3+}$ ions exhibit strong emission in the visible domain, the most intense corresponding to $^4G_{5/2} \rightarrow ^6H_{7/2}$ transition at 612 nm for Sm: $Sc_2O_3$ [34], at 610 nm for Sm: $Y_2O_3$ [36], 617 nm for Sm: YAG [30, 31], 593 nm for Sm: $SrAl_{12}O_{19}$ [32, 33].

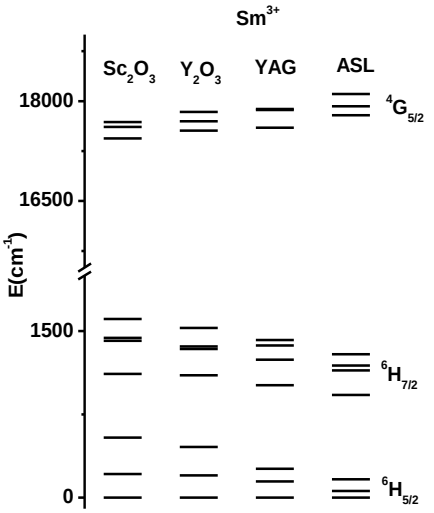


*Fig. 4 Partial energy level scheme of $Sm^{3+}$ in oxides.*

## 3. Conclusion

The correlation between structure and composition of different oxides and the energy levels of the $Nd^{3+}$ and $Sm^{3+}$ , as active ions, was analyzed. These systems are interesting for visible emission in orange by direct excitation of $Sm^{3+}$ ions and in blue from $Nd^{3+}$ laser emissions in the ~ 900 nm range by doubling. The chosen hosts are sesquioxides $Sc_2O_3$, $Y_2O_3$, garnets- YAG and hexaaluminates $Sr_{1-x}Nd_yLa_{x-y}Mg_xAl_{12-x}O_{19}$, oxides differing strongly by structure or composition (CN- near neighbor oxygen coordination numbers, local symmetry, cation - ion and cation – cation distances, etc).

The energies of the barycenters of the manifolds were taken as a measure of the nephelauxetic effect; they increase from $Sc_2O_3$ to ASL (Tables 2, 3), leading to emissions at decreasing wavelengths The structural and compositional factors influence on the crystal field splitting of the laser levels of Nd (Fig. 2) and $Sm^{3+}$ (Fig. 4) are analyzed in terms of the scalar crystal field strength parameter and maximum splitting of the manifolds. It is shown that $Nd^{3+}$ emission range is controlled not only by the nephelauxetic effect, but also by the crystal field strength giving the maximum splitting of $^4I_{9/2}$ level.

**Acknowledgements**

This work was supported by CNCSIS –UEFISCSU, project number PNII – Human Resources PD-160/2010.

## References

[1] C. K. Jörgensen, "Absorption spectra and chemical bonding in complexes", The Pergamon Press, Ltd., London. (1964).
[2] R. C. Powell, Physics of Solid-State Laser Materials, AIP Press-Springer (1998).
[3] A. A. Kaminskii, Crystalline Lasers: Physical Processes and Operating Schemes, CRC Press, 1996.
[4] M. Faucher, D. Garcia, O. K. Moune, J. Luminescence, **51**, 341 (1992).
[5] L. Fornasiero, E. Mix, V. Peters, E. Heumann, K. Petermann, G. Huber, OSA Trends in Optics and Photonics: Advanced Solid State Lasers, Vol. **26**, M. M. Fejer, H. Injeyan, U. Keller, Eds. (1999), p. 249.
[6] B. M. Walsh, J. M. McMahon, W. C. Edwards, N. P. Barnes, R. W. Equal, R. L. Hutchinson, JOSA B **19**, 2893 (2002).
[7] V. Lupei, G. Aka, D. Vivien, Opt. Commun. **204**, 399 (2002).
[8] S. Strohmaier, H. Eichler, J. F. Bisson, H. Yagi, K. Takaichi, K. Ueda, T. Yanagitani, A. A. Kaminskii, Laser Physics Letters **2**, 383 (2005)
[9] C. Zhang, X. Zhang, Q. Wang, Z. Cong, S. Fan, X. Chen, Z. Liu, Z. Zhang, Laser Physics Letters, **6**, 521 (2009).
[10] G. Aka, D. Vivien, V. Lupei, Appl. Phys. Lett. **85**, 2685 (2004).
[11] V. Lupei, G. Aka, D. Vivien, Optics Letters **31**, 1064 (2006).
[12] R. W. G. Wickoff, "Crystal structure", Vol. **3** Inorganic Compounds (Interscience Publishers Inc.) 1965.
[13] R. D. Shannon, Acta Crystallographica **A32**, 751 (1976).
[14] V. Lupei, A. Lupei, S. Georgescu, B. Diaconescu, T. Taira, Y. Sato, S. Kurimura, A. Ikesue, J. Opt. Soc. Amer. B **19**, 360 (2002).
[15] J. B. Gruber, D. K. Sardar, R. M. Yow, T. H. Allik, B. Zandi, J. Appl. Phys **96**, 3050 (2004).
[16] A. Lupei, V. Lupei, T. Taira, Y. Sato, A. Ikesue, C. Gheorghe, J. Luminescence, **102-103**, 72, (2003).
[17] J.B.Gruber, D.K. Sardar, K. L. Nash, R. M. Yow, J. Appl. Phys, **102**, 023103 (2007).
[18] V. Lupei, A. Lupei, A. Ikesue, Appl. Phys. Lett. **86**, 111118 (2005).
[19] V. Lupei, A. Lupei, A. Ikesue, Optical Materials **30**, 1781 (2008).
[20] V. Peters, "Growth and Spectroscopy of Ytterbium-Doped Sesquioxides", Dissertation thesis, Institute of Laser-Physics, University of Hamburg, Germany, (2001).
[21] D. Vivien, G. Aka, A. Lupei, V. Lupei, C. Gheorghe, Proc. SPIE **5581**, 287 (2004).
[22] A. Lupei, V. Lupei, C. Gheorghe, D. Vivien, G. Aka, P. Ascheoung, J. Appl. Phys., **96**(6), 3057 (2004).
[23] J. F. Wyart, A. Meftah, A. Bachelier, J. Sinzelle, W. L. Tchang-Brillet, N. Champion, N. Spewctor, J. Sugar, J. Phys. B: At. Mol. Opt. Phys. **39**, L77, (2006).
[24] E. Antic –Fidancev, J. Alloys and Compounds **300-301**, 2 (2000).
[25] A. Lupei, Antic-Fidancev, G. Aka, D. Vivien, P. Aschehoug, Ph. Goldner, F. Pelle, L. Gheorghe, Phys. Rev. B. 65, 224518 (2002).
[26] F. Auzel, Materials Research Bulletin **14**, 223 (1979).
[27] C. A. Morrison, D. E. Wortman, N. Karayianis, J. Phys. C: Solid State Phys., **9**, L191 (1976).
[28] A. Lupei, V. Lupei, C. Gheorghe, L. Gheorghe, D. Vivien, G. Aka and E. Antic - Fidancev, J. Phys. Cond. Matter, **18**, 597 (2006).
[29] J. F. Martel, S. Jandl, B. Viana, D. Vivien, J. Phys. Chem. Solid **61,** 1455 (2000).
[30] J. B. Gruber, E. Hills, P. Nadler, M. R. Kokta, C A. Morrison, Chem. Phys., **113**, 175 (1987).
[31] M. Malinowski, R. Wolski, Z. Frukacz, T. Lukasiewicz, Z. Luczynski, J. Appl. Spectrosc., **62**, 839 (1995).
[32] A. Lupei, V. Lupei, C. Gheorghe, A. Ikesue, Romanian Reports in Physics, **63**, 817 (2011).
[33] Vijay Singh, Jun-Jie Zhu, V. Natarajan, Phys. Stat. Sol. (a) **203**, 2058 (2006).
[34] C. Gheorghe, A. Lupei, L. Gheorghe, A. Achim, Optoelectron. Adv. Mater. - Rapid Commun. **5**(2), 116 (2011).
[35] C. Gheorghe, A. Lupei, F. Voicu, Optoelectron. Adv. Mater. - Rapid Commun. **6** (1-2), 49 (2012).
[36] C. A. Kodaira, R. Stefani, A. S. Maia, M. C. F. C. Felinto, H. F. Brito, J. Luminescence, **127,** 616 (2007).

*Corresponding author: cristina_gheorghe2002@yahoo.com